

Highly Accurate Description of Long-Range Interactions through the Combination of Neural Networks and Physical Models

Yingyue Hong,^{†,‡} Jiayu Huang,^{*,¶,†} and Dong H. Zhang^{*,†,‡}

[†]*State Key Laboratory of Molecular Reaction Dynamics, Dalian Institute of Chemical Physics, Chinese Academy of Science, Dalian 116023, China*

[‡]*School of Chemical Sciences, University of Chinese Academy of Sciences, Beijing 100049, China*

[¶]*Department of Physics, Dalian University of Technology, Dalian 116024, China*

E-mail: jyhuang@dlut.edu.cn; zhangdh@dicp.ac.cn

Abstract

We present a simple and general way to accurately describe long-range interactions between atoms and molecules through combining neural networks with physical models. Demonstrations on the H_3 , Li_3 and $2K\text{Rb}$ systems illustrate the exceptional extrapolation capabilities of the trained model, supported by underlying physical models. More importantly, the model exhibits high accuracy at energy scales below a few hundred millikelvin, where the reliability of *ab initio* methods diminishes.

Understanding and manipulating ultracold collisions ($T < 10^{-3}$ K) between atoms and molecules has become a forefront in the fields of physics and chemistry, with implications ranging from quantum information processing,¹⁻⁴ precision measurement,^{5,6} and quantum control of chemical reactions.⁷⁻¹⁰

At ultracold temperatures, particles possess minimal kinetic energy. Due to their slow movement, long-range interactions between these particles become dominant. These interactions, extending over significant distances, play a crucial role in shaping particle behavior and notably influence the outcomes of ultracold collisions. Consequently, creating accurate models to represent long-range interactions is essential for the understanding of quantum dynamics during ultracold collisions. Yet, achieving the necessary precision on a scale as small as several nanokelvins presents challenges for the accuracy of potential energy calculations—a difficulty that current *ab initio* methods may find challenging to overcome.

An alternative approach is employing physics-motivated analytical models to describe long-range interactions. In these models, the long-range behavior of adiabatic Born-Oppenheimer potentials is commonly expressed as a power series in terms of $1/R$, where R represents the distance between the interacting particles. Guided by high-resolution spectrum experiments, achieving an accurate representation of long-range interactions can be accomplished through finely tuning parameters within physical models. This method has proven successful in the study of ultracold atoms.¹¹ It has also been shown that physical models can be applied for representing long-range interactions between ultracold closed-shell molecules by using the standard long-range expansion,^{12–14} which includes multipole-multipole electrostatic, dispersion, and induction interactions. However, these analytical models often face challenges when attempting to represent the intricate long-range interactions within ultracold open-shell molecules.

Recent advancements in artificial neural networks (NNs) introduced a powerful tool for modeling chemical systems. The NN-based potential models can estimate interaction energies with near *ab initio* accuracy while drastically reducing computational costs by orders of magnitude.^{15–23} However, the incorporation of artificial neural networks faces notable limitations when applied to systems influenced by long-range interactions. Firstly, its capacity to extrapolate beyond available data points is restricted, potentially introducing inaccuracies in describing interactions over very long distances. Secondly, the accuracy of the NN method is limited by its reliance on *ab initio* points. To overcome these challenges, there is a recent trend in the scientific community to

combine neural network methods with physics models.^{24–28} However, the majority of efforts have been concentrated on enhancing neural network performance by incorporating physical models. The intrinsic challenges of extrapolation and accuracy mentioned above have not been effectively resolved. Consequently, there is currently a shortage of potential energy surface (PES) capable of offering an accurate description of long-range interactions for ultracold collisions.

In this paper, we present a new way to accurately describe long-range interactions between atoms and molecules. The method combines neural networks with physical models, offering a simple and general solution. Demonstrations on the H_3 , Li_3 and 2KRb systems illustrate the exceptional extrapolation capabilities of the trained model, supported by underlying physical models. Moreover, the model exhibits superior accuracy at energy scales below a few hundred millikelvin, where the reliability of ab initio points becomes uncertain.

We start by considering the Jacobi coordinates for a triatomic system A+BC, denoted as (R, r, θ) . Here, R represents the distance from A to the center of mass of BC, r is the bond length within BC, and θ is the angle between R and r . According to perturbation theory, the system energy can be expressed

$$V(R, r, \theta) = U(r) + u_{LR}(R, r, \theta) \tag{1}$$

This energy is divided into two components: $U(r)$, representing the inner energy of molecule as the distance R goes to infinity, and $u_{LR}(R, r, \theta)$, which characterizes the long-range interaction energy. The long-range interaction energy can be further expanded as a summation of terms with inverse powers of R :

$$u_{LR}(R, r, \theta) = - \sum_i \frac{C_{m_i}(r, \theta)}{R^{m_i}} \tag{2}$$

where $C_{m_i}(r, \theta)$ denotes coefficients that depend on r and θ . The values of m_i need to be adjusted based on the physical characteristics of specific system.

The very idea of this study is to introduce neural networks to represent $C_{m_i}(r, \theta)$. The advantage of neural networks in accurately approximating non-linear functions provides increased flexibility for handling complex expressions of $C_{m_i}(r, \theta)$. To implement this concept, we adopted

feed-forward multilayer networks for the construction of $C_{m_i}(r, \theta)$. These networks comprise an input layer, several hidden layers, and an output layer. Input data undergoes processing as it forwards through the hidden layers, with each element from the previous layer connecting to every component in the subsequent layer through suitable weight coefficients. The entire process is mathematically described by

$$n_i^m = \sum_{j=1}^{S^{m-1}} \left(w_{i,j}^m a_j^{m-1} \right) + b_i^m \quad (3)$$

$$a_i^m = f^m(n_i^m) \quad (4)$$

in which n_i^m stands for the net input of neuron i in the m -th layer, a_i^m represents the output of neuron i in the m -th layer activation functions. Commonly used functions to denote activation functions f^m include hyperbolic tangent, linear function, and logistic. $w_{i,j}^m$ denotes the weight at row i and column j between layer $m-1$ and layer m . b_i^m represents the bias of neuron i in layer m .

The illustration in Figure 1 shows the neural network structure. The input layer of the neural network consists of \vec{r}_i , $\vec{\theta}_i$, and $\vec{\phi}_j$, while the output layer is C_{m_i} . Once C_{m_i} is obtained, the calculation of u_{LR} follows using Eq (2). Therefore, The formulation of the loss function P can be expressed as:

$$P = \frac{1}{Q} \sum_{q=1}^Q \left(u_{LR}^{q,(ab\ intio)} - u_{LR}^{q,(fit)} \right)^2 \quad (5)$$

The objective is to minimize the loss function through the Levenberg-Marquardt algorithm iteration. Notably, the input layer of neural network does not include R due to the independence of C_{m_i} from R . Instead, R is passed as a parameter to the internal optimization process of the neural network. Hence, the Jacobian matrix can be expressed as:

$$\frac{\partial e(\vec{w})}{\partial w_j} = - \sum_{i=0}^{last} \frac{1}{R^{m_i}} \frac{\partial C_{m_i}}{\partial w_j} \quad (6)$$

While we use the 3-atom collision system in Jacobi coordinates as an example, it is important to note that this is a general method that can be extended to any coordinate system and dimension.

We applied the new method to the simplest triatomic collision system: H+H₂. The system is an ideal choice for testing the accuracy of PES, as *ab initio* calculations can provide the most accurate results for it. The *ab initio* data were calculated through the Molpro program²⁹ by using the UCCSD-T method^{30,31} at the aug-cc-pv5z level.³² We perform calculations at 2249 points, ranging from 9.6 to 18.3 bohr for R and 1.0 to 4.0 bohr for r . The neural network structure employed was 2-30-3, with the values of m_i chosen as 6, 8, and 10 to represent the long-range interaction. The activation functions are logsig and line, and the testing set comprises 20% of the data. To ensure the reliability of the *ab initio* points, most of training points is refined to energies higher than 0.05 cm⁻¹. The obtained root-mean-square error (RMSE) was 0.00209 cm⁻¹. Figure 2(A) shows the distribution of errors of the fitting results for the long-range potential energy of H₃ system. It is clear that the errors tend to stay around 10⁻³ cm⁻¹, showing that our fitting is quite accurate. All points have a relative error less than 10%, and a large majority (86.62%) have a relative error less than 1%. Figure 2(B) illustrates the variation of the long-range interaction u_{LR} with the distance between the H atom and H₂ molecule at a specific configuration. The energy values are calculated from fitting results, *ab initio* methods, and the well-known BKMP2 PES. It is evident that the value of *ab initio* points become unreliable at energy below 10⁻² cm⁻¹. In contrast, our model shows robust extrapolation capabilities, yielding accurate values over extended distances. This demonstrates that the new method overcomes the inherent challenges associated with extrapolation and accuracy in pure neural network methods, and has strong potential to be used for ultracold collisions studies.

Ultracold molecule collision experiments primarily focus on collisions involving alkali metal molecules. To show the capability of our method in describing the long-range interaction of alkali metal molecules systems, we applied it to model the Li+Li₂ collision. We employed Molpro program with the UCCSD-T/AVTZ method^{30,31,33} to calculate 2669 points, with R ranging from 20 to 40 bohr and r from 4.0 to 9.4 bohr. The neural network structure is 2-50-3, and the output layer consists of C₆, C₈, and C₁₀. The activation functions are logsig and line, and the testing set comprises 10% of the data. The testing set comprises 10% of the data. Most of training

points is refined to energies higher than 0.05 cm^{-1} , results in a RMSE of 0.0346 cm^{-1} . The comparison between Figure 2(B) and Figure 3(B) reveals that the long-range interaction between Li and Li_2 is considerably stronger than that between H and H_2 at the same distance, showing the importance of accurate long-range PES. From Figure 3(A), it is clear that the errors stabilize around 0.01 cm^{-1} , with the relative error of fitting results exceeding 10% at energies below 0.1 cm^{-1} . However, we attribute this error to the unreliability of *ab initio* calculations rather than our model. This interpretation is supported by Figure 3(B), which indicates that *ab initio* calculations become unreliable at energy levels below 0.1 cm^{-1} . Therefore, it is reasonable to conclude that the accuracy of the *ab initio* method is limited to 0.1 cm^{-1} for the Li_3 system. This agrees with recent experimental evidence, indicating challenges even for the gold standard *ab initio* method in providing accurate intermolecular potentials at energy levels of several cm^{-1} .³⁴ On the contrary, our model demonstrates strong extrapolation capabilities, accurately predicting values over a wide range of intermolecular distances, showing its reliability for various systems.

To show the applicability of the new method to higher-dimensional systems, we applied it to the 2KRb system, which is the most widely studied ultracold molecule-molecule collision system and can be denoted in the Jacobi coordinates as $(R, r_1, r_2, \theta_1, \theta_2, \phi)$. Recently, Huang and her coworkers developed an analytical long-range PES for the long-range interaction of $\text{KRb}+\text{KRb}$ collisions.¹³ We randomly selected 29,706 points from the newly developed long-range PES, with R ranging from 16 bohr to 64 bohr and two r values ranging from 5.67 to 8.87. The neural network structure is 5-400-4, and the output layer consists of C_3 , C_4 , C_5 , and C_6 , guided by the formula used to construct the analytical PES. The activation functions are logsig and line, and the testing set comprises 10% of the data. As shown in Figure 4(A), nearly all points (97.86%) have a relative error less than 10%, and a large majority (79.95%) have a relative error less than 1%, resulting a RMSE of 0.0244 cm^{-1} . More interestingly, Figure 4(B) illustrates that the trained model accurately predicts results for collision configurations even in the absence of sampling over distances up to 1000 bohr. This demonstrates that our method inherits the strong non-linear fitting capability of NN methods. Therefore, this method is well suitable for higher-dimensional systems. We

are confident that the new method has the potential to perform effectively in the investigation of ultracold molecule-molecule collisions, a subject currently of great interest.

To summarize, a simple and general method is developed for describing long-range interactions between atoms and molecules by combining neural networks with physical models. Tests on the H_3 , Li_3 , and $2KRb$ systems demonstrate that this method has strong extrapolation capabilities and accuracy over very long distances. This illustrates that the new method overcomes the inherent challenges associated with extrapolation and accuracy in pure neural network methods, showing its strong potential for use in the study of ultracold collisions.

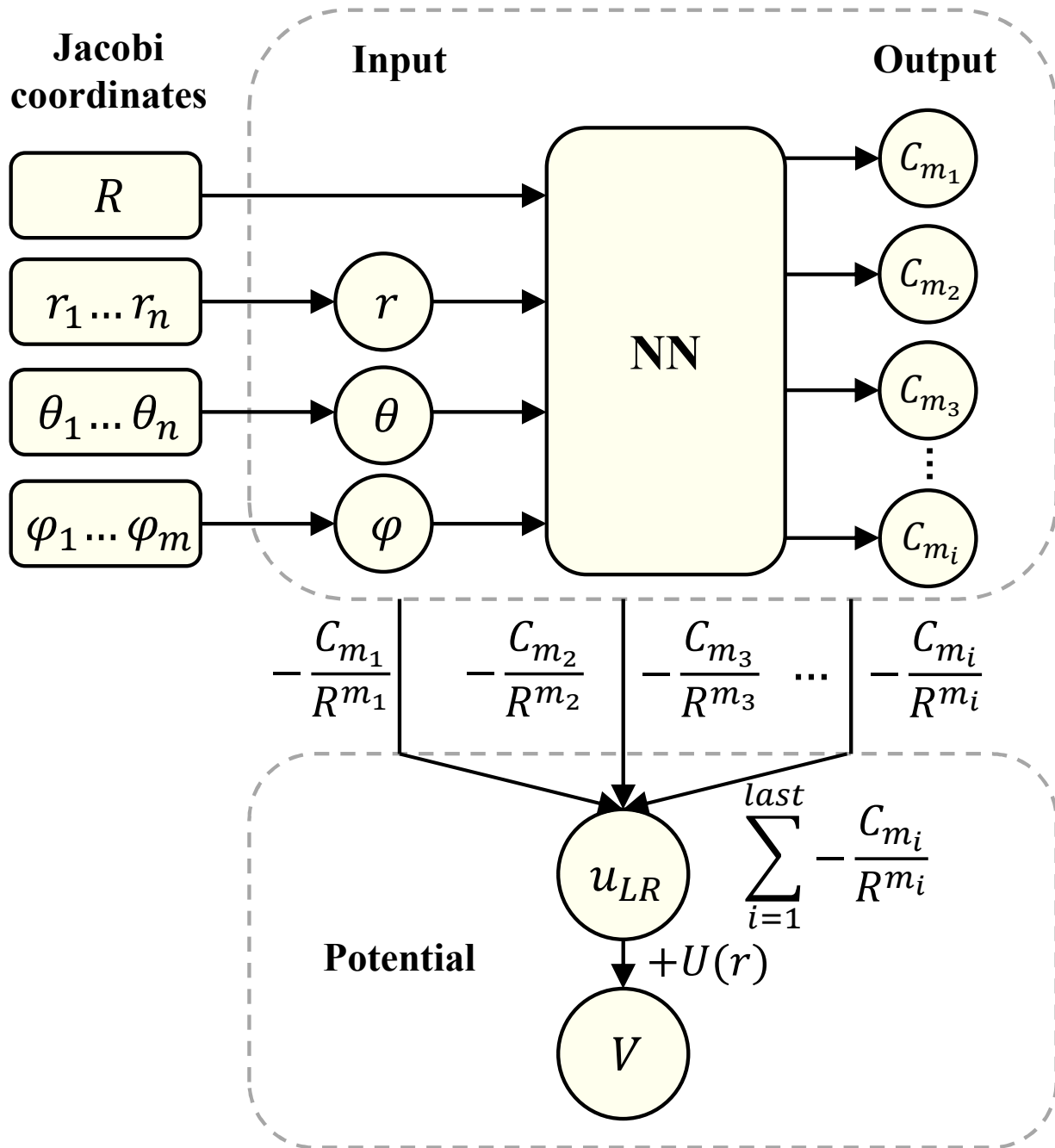


Figure 1: The schematic diagram illustrates the fitting process for long-range interaction. The initial step involves processing the Jacobi coordinates of the system. r , θ and φ are normalized and included as input layers in the neural network. Following the fitting process through the neural network, we obtain values for C_{m_i} . These parameters are then utilized to calculate u_{LR} . With these acquired values, the potential energy in the long-range region is determined by adding the inner energy $U(r_i)$ of molecules to u_{LR} .

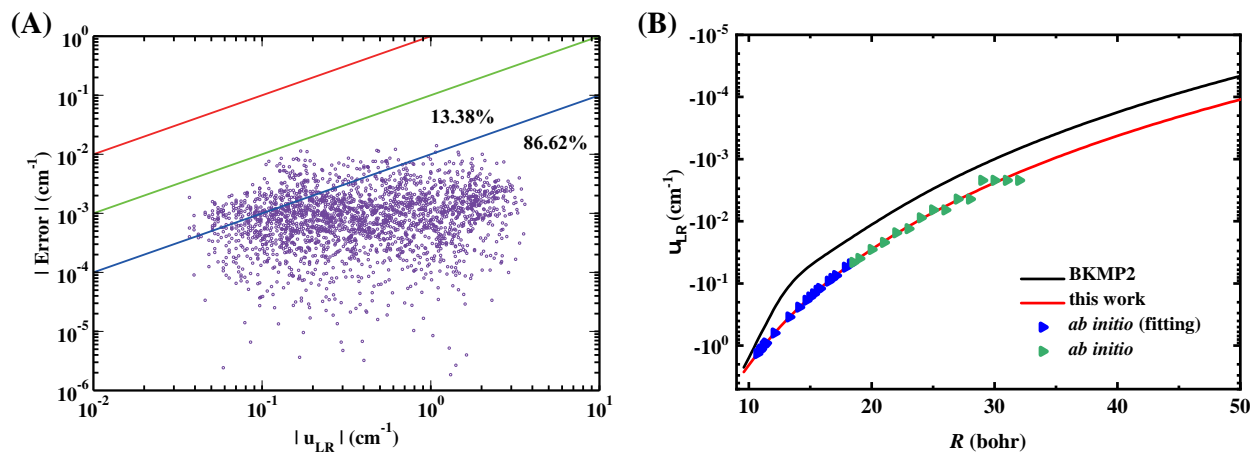


Figure 2: (A) Plot of the distribution of errors in the ground state potential energy surface (PES) for the H_3 system. The *ab initio* potential energy is plotted on the horizontal axis, while the absolute error is represented on the vertical axis. The red, green, and blue lines divide the points into regions with errors exceeding 100%, 10%, and 1%, respectively. Each region is labeled with the corresponding percentage of error points; (B) One-dimensional plot of u_{LR} energies calculated from fitting results, *ab initio* methods, and BKMP2 PES. The plot is generated at $\theta = 90^\circ$ and the equilibrium bond length ($r = 1.4$ Bohr).

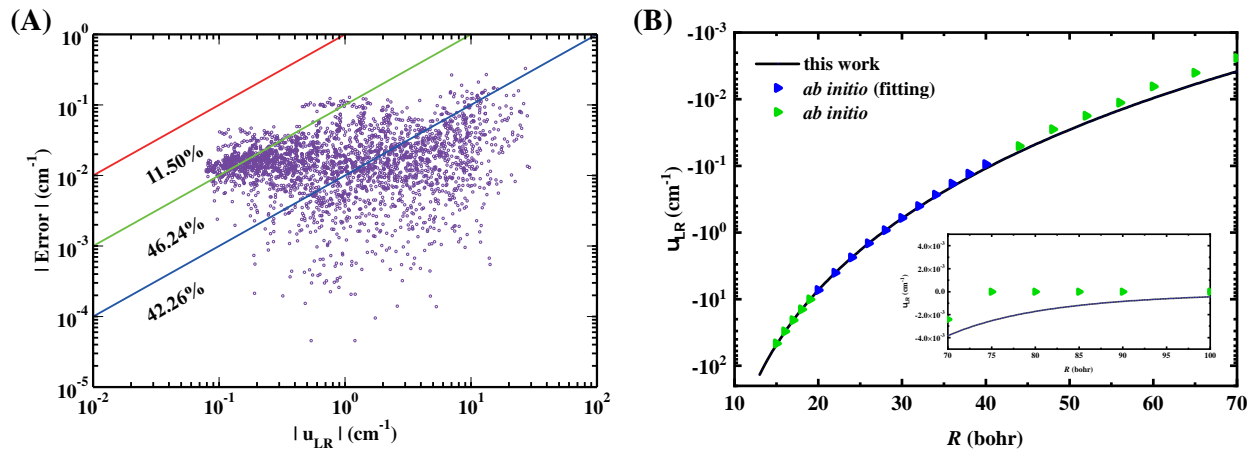


Figure 3: (A) Plot of the distribution of errors in the ground state potential energy surface for the Li_3 system, similar to the representation in Figure 2(A); (B) One-dimensional plot of u_{LR} energies calculated from fitting results compared with *ab initio* methods. The plot is generated at $\theta = 90^\circ$ and the equilibrium bond length ($r = 5.2$ Bohr). The inset shows the results over extended distance.

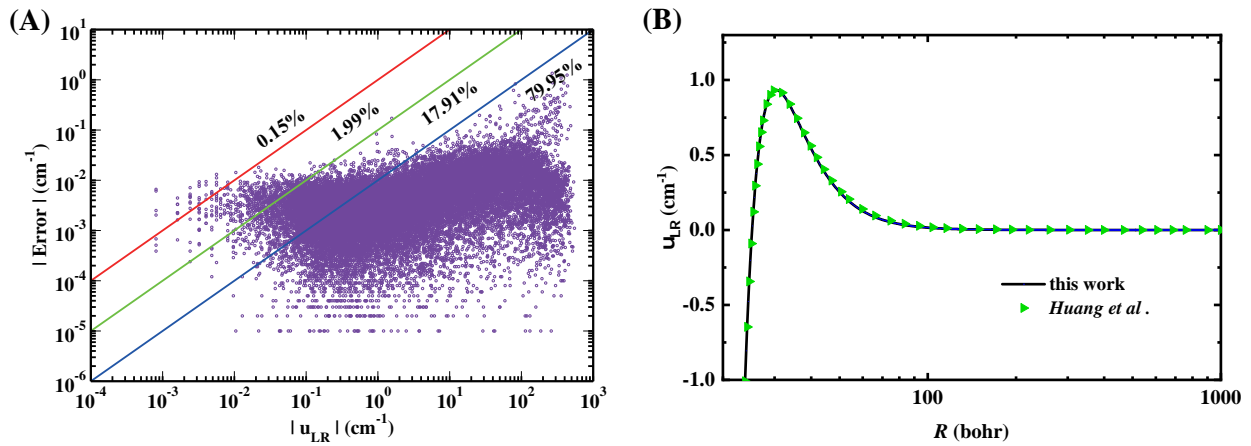


Figure 4: (A) Plot of the distribution of errors in the ground state potential energy surface for the KRB+KRB system, similar to the representation in Figure 2(A); (B) One-dimensional plot of u_{LR} energies calculated from fitting results and the analytical PES constructed by Huang and her coworkers. The plot is generated at $\theta_1 = 90^\circ$, $\theta_2 = 90^\circ$, $\phi = 0^\circ$, and the equilibrium bond length ($r_1 = r_2 = 7.66$ Bohr).

References

- (1) Kaufman, A. M.; Ni, K. K. Quantum science with optical tweezer arrays of ultracold atoms and molecules. *Nat. Phys.* **2021**, *17*, 1324–1333.
- (2) Jenkins, A.; Lis, J. W.; Senoo, A.; McGrew, W. F.; Kaufman, A. M. Ytterbium Nuclear-Spin Qubits in an Optical Tweezer Array. *Phys. Rev. X* **2022**, *12*, 021027.
- (3) González-Cuadra, D.; Zache, T. V.; Carrasco, J.; Kraus, B.; Zoller, P. Hardware Efficient Quantum Simulation of Non-Abelian Gauge Theories with Qudits on Rydberg Platforms. *Phys. Rev. Lett.* **2022**, *129*, 160501.
- (4) Hu, M. G.; Liu, Y.; Nichols, M. A.; Zhu, L.; Quémener, G.; Dulieu, O.; Ni, K. K. Nuclear spin conservation enables state-to-state control of ultracold molecular reactions. *Nat. Chem.* **2021**, *13*, 435–440.
- (5) Liu, Y.; Hu, M. G.; Nichols, M. A.; Yang, D.; Xie, D.; Guo, H.; Ni, K. K. Precision test of statistical dynamics with state-to-state ultracold chemistry. *Nature* **2021**, *593*, 379–384.
- (6) Christakis, L.; Rosenberg, J. S.; Raj, R.; Chi, S.; Morningstar, A.; Huse, D. A.; Yan, Z. Z.; Bakr, W. S. Probing site-resolved correlations in a spin system of ultracold molecules. *Nature* **2023**, *614*, 64–69.
- (7) Zhao, B.; Pan, J.-W. Quantum control of reactions and collisions at ultralow temperatures. *Chem. Soc. Rev.* **2022**, *51*, 1685–1701.
- (8) Liu, Y.; Ni, K.-K. Bimolecular Chemistry in the Ultracold Regime. *Annu. Rev. Phys. Chem.* **2022**, *73*, 73–96.
- (9) Tobias, W. G.; Matsuda, K.; Li, J.-R.; Miller, C.; Carroll, A. N.; Bilitewski, T.; Rey, A. M.; Ye, J. Reactions between layer-resolved molecules mediated by dipolar spin exchange. *Science* **2022**, *375*, 1299–1303.

- (10) Yang, H.; Wang, X. Y.; Su, Z.; Cao, J.; Zhang, D. C.; Rui, J.; Zhao, B.; Bai, C. L.; Pan, J. W. Evidence for the association of triatomic molecules in ultracold $^{23}\text{Na}^{40}\text{K} + ^{40}\text{K}$ mixtures. *Nature* **2022**, *602*, 229–233.
- (11) Jones, K. M.; Tiesinga, E.; Lett, P. D.; Julienne, P. S. Ultracold photoassociation spectroscopy: Long-range molecules and atomic scattering. *Rev. Mod. Phys.* **2006**, *78*, 483–535.
- (12) Yang, D.; Huang, J.; Hu, X.; Xie, D.; Guo, H. Statistical quantum mechanical approach to diatom–diatom capture dynamics and application to ultracold $\text{KRb} + \text{KRb}$ reaction. *J. Chem. Phys.* **2020**, *152*, 241103.
- (13) Huang, J.; Yang, D.; Zuo, J.; Hu, X.; Xie, D.; Guo, H. Full-Dimensional Global Potential Energy Surface for the $\text{KRb} + \text{KRb} \rightarrow \text{K}_2\text{Rb}_2^* \rightarrow \text{K}_2 + \text{Rb}_2$ Reaction with Accurate Long-Range Interactions and Quantum Statistical Calculation of the Product State Distribution under Ultracold Conditions. *J. Phys. Chem. A* **2021**, *125*, 6198–6206.
- (14) Buren, B. A neural network potential energy surface for the $\text{Li} + \text{LiNa} \rightarrow \text{Li}_2 + \text{Na}$ reaction and quantum dynamics study from ultracold to thermal energies. *Phys. Chem. Chem. Phys.* **2023**, *25*, 19024–19036.
- (15) Blank, T. B.; Brown, S. D.; Calhoun, A. W.; Doren, D. J. Neural network models of potential energy surfaces. *J. Chem. Phys.* **1995**, *103*, 4129–4137.
- (16) Brown, D. F. R.; Gibbs, M. N.; Clary, D. C. Combining ab initio computations, neural networks, and diffusion Monte Carlo: An efficient method to treat weakly bound molecules. *J. Chem. Phys.* **1996**, *105*, 7597–7604.
- (17) Handley, C. M.; Popelier, P. L. A. Potential Energy Surfaces Fitted by Artificial Neural Networks. *J. Phys. Chem. A* **2010**, *114*, 3371–3383.
- (18) Behler, J. Neural network potential-energy surfaces in chemistry: a tool for large-scale simulations. *Phys. Chem. Chem. Phys.* **2011**, *13*, 17930–17955.

- (19) Chen, J.; Xu, X.; Xu, X.; Zhang, D. H. Communication: An accurate global potential energy surface for the $\text{OH} + \text{CO} \rightarrow \text{H} + \text{CO}_2$ reaction using neural networks. *J. Chem. Phys.* **2013**, *138*, 221104.
- (20) Jiang, B.; Guo, H. Permutation invariant polynomial neural network approach to fitting potential energy surfaces. *J. Chem. Phys.* **2013**, *139*, 054112.
- (21) Liu, T.; Zhang, Z.; Fu, B.; Yang, X.; Zhang, D. H. A seven-dimensional quantum dynamics study of the dissociative chemisorption of H_2O on $\text{Cu}(111)$: effects of azimuthal angles and azimuthal angle-averaging. *Chem. Sci.* **2016**, *7*, 1840–1845.
- (22) Shao, K.; Chen, J.; Zhao, Z.; Zhang, D. H. Communication: Fitting potential energy surfaces with fundamental invariant neural network. *J. Chem. Phys.* **2016**, *145*, 071101.
- (23) Shakouri, K.; Behler, J.; Meyer, J.; Kroes, G.-J. Accurate Neural Network Description of Surface Phonons in Reactive Gas–Surface Dynamics: $\text{N}_2 + \text{Ru}(0001)$. *J. Phys. Chem. Lett.* **2017**, *8*, 2131–2136.
- (24) Anstine, D. M.; Isayev, O. Machine Learning Interatomic Potentials and Long-Range Physics. *J. Phys. Chem. A* **2023**, *127*, 2417–2431.
- (25) Tu, N. T. P.; Rezaiooei, N.; Johnson, E. R.; Rowley, C. N. A neural network potential with rigorous treatment of long-range dispersion. *Digital Discovery* **2023**, *2*, 718–727.
- (26) Unke, O. T.; Meuwly, M. PhysNet: A Neural Network for Predicting Energies, Forces, Dipole Moments, and Partial Charges. *J. Chem. Theory Comput.* **2019**, *15*, 3678–3693.
- (27) Zhang, L.; Wang, H.; Muniz, M. C.; Panagiotopoulos, A. Z.; Car, R.; E, W. A deep potential model with long-range electrostatic interactions. *J. Chem. Phys.* **2022**, *156*, 124107.
- (28) Li, Y.; Zhai, Y.; Li, H. MLRNet: Combining the Physics-Motivated Potential Models with Neural Networks for Intermolecular Potential Energy Surface Construction. *J. Chem. Theory Comput.* **2023**, *19*, 1421–1431.

- (29) Werner, H.-J.; Knowles, P. J.; Knizia, G.; Manby, F. R.; Schütz, M. Molpro: a general-purpose quantum chemistry program package. *WIREs Comput. Mol. Sci.* **2012**, *2*, 242–253.
- (30) Deegan, M. J.; Knowles, P. J. Perturbative corrections to account for triple excitations in closed and open shell coupled cluster theories. *Chem. Phys. Lett.* **1994**, *227*, 321–326.
- (31) Knowles, P. J.; Hampel, C.; Werner, H.-J. Erratum: “Coupled cluster theory for high spin, open shell reference wave functions” [*J. Chem. Phys.* *99*, 5219 (1993)]. *J. Chem. Phys.* **2000**, *112*, 3106–3107.
- (32) Dunning, J., Thom H. Gaussian basis sets for use in correlated molecular calculations. I. The atoms boron through neon and hydrogen. *J. Chem. Phys.* **1989**, *90*, 1007–1023.
- (33) Prascher, B. P.; Woon, D. E.; Peterson, K. A.; Dunning, T. H.; Wilson, A. K. Gaussian basis sets for use in correlated molecular calculations. VII. Valence, core-valence, and scalar relativistic basis sets for Li, Be, Na, and Mg. *Theor. Chem. Acc.* **2011**, *128*, 69–82.
- (34) Vogels, S. N.; Karman, T.; Kłos, J.; Besemer, M.; Onvlee, J.; Van Der Avoird, A.; Groenenboom, G. C.; Van De Meerakker, S. Y. Scattering resonances in bimolecular collisions between NO radicals and H₂ challenge the theoretical gold standard. *Nat. Chem.* **2018**, *10*, 435–440.

TOC Graphic

